
The Ultraviolet Spectrum of B-Type Supergiants

Anne B. Underhill

Phil. Trans. R. Soc. Lond. A 1975 **279**, 429-442

doi: 10.1098/rsta.1975.0077

Email alerting service

Receive free email alerts when new articles cite this article - sign up in the box at the top right-hand corner of the article or click [here](#)

The ultraviolet spectrum of B-type supergiants

BY ANNE B. UNDERHILL

Goddard Space Flight Center, Greenbelt, Maryland, U.S.A.

The broad, steep-sided absorption lines in B-type supergiant spectra are stronger than the absorption lines in main-sequence stars. In addition to lines from the second, third and fourth spectra of the light elements and the metals there is a broad, pointed feature at 1720 Å which has constant strength in the B-type supergiants regardless of spectral type. The complete identification of this blend is not known. At high resolution the ultraviolet resonance lines of C iv, N v, Si iii and Si iv in the spectra of OB supergiants are shortward displaced by velocities up to 1800 km s⁻¹ indicating the presence of an escaping atmosphere. At type B5 the expanding atmosphere is moving at about 120 km s⁻¹ which means that the material is probably brought to rest before it escapes from the star. Evidence is presented of the presence of a stationary shell around the B5Ia supergiant η Canis Majoris as well as a slowly expanding atmosphere.

1. INTRODUCTION

In the spectral region accessible to ground-based telescopes the spectra of B-type supergiants are distinguished by the presence of broad, sharp-sided absorption lines and the absence of strong Stark broadened wings on the hydrogen and helium lines. The lines, except those of hydrogen and helium, are stronger than in the main-sequence stars of similar spectral type. This strength is a characteristic feature of high luminosity which together with the lack of strong Stark broadened wings on the hydrogen and helium allows immediate recognition of supergiant spectra. This type of behaviour carries over into the ultraviolet spectral region.

OAO-2 spectrum scans of five early-type main-sequence stars and the shell star ζ Tauri are shown in figure 1. The very strong absorption line is Lyman α of hydrogen which is partly stellar and partly interstellar in origin. Twenty absorption features can be detected. The most prominent are line 9 due chiefly to C iv, line 14 due chiefly to Si iv, line 17 due chiefly to Si iii and line 18 due partly to Si ii. At 10 Å resolution there are few distinctive features in main-sequence spectra. OAO-2 spectrum scans of six early-type supergiants are shown in figure 2. The separate absorption features except that due to hydrogen are stronger and more definite than in the main-sequence spectra, the resonance lines due to C iv and Si iv being particularly strong at types B1 and B0. In addition, there is a broad, pointed feature at 1720 Å which has constant strength in the supergiants, regardless of spectral type. This feature appears in the spectrum of the shell star ζ Tauri, but not in the spectra of main-sequence stars. It is an unusual feature in that the intensity remains roughly constant from type B0Ia to B8Ia. Lines of Ni iii, Al ii and Fe ii probably contribute to this blend, as is shown by Sara Heap's high resolution observation of this feature in ζ Tauri, but it would be most fortuitous if these lines so change in strength with decreasing temperature that the blended feature remains unchanged. At present this feature must be considered to be unidentified.

Ultraviolet spectra of OB supergiants have been obtained by Morton, Jenkins & Bohlin (1968) at about 1 Å resolution using a rocket-borne spectrograph. These spectra show numerous strong, steep-sided absorption lines. In the bright giant δ Orionis and the supergiants ε Orionis

and ζ Orionis the ultraviolet resonance lines of C IV, N V, Si III and Si IV, as well as the C III blend at 1176 Å are present as absorption lines shifted shortward of their laboratory wavelengths with velocities up to 1800 km s⁻¹. The C IV and Si IV lines have emission components at their longward edges in all three luminous stars. These observations definitely show that an OB supergiant is surrounded by an atmosphere which is moving outward at a velocity greater than the velocity of escape. Such an expanding atmosphere is not visible in the part of the spectrum of B-type supergiants accessible to ground-based telescopes (Lamers 1972; Van Helden 1972; Underhill & Fahey 1973) although it is shown by faint broad emission features in the spectra of luminous O stars (Wilson 1958).

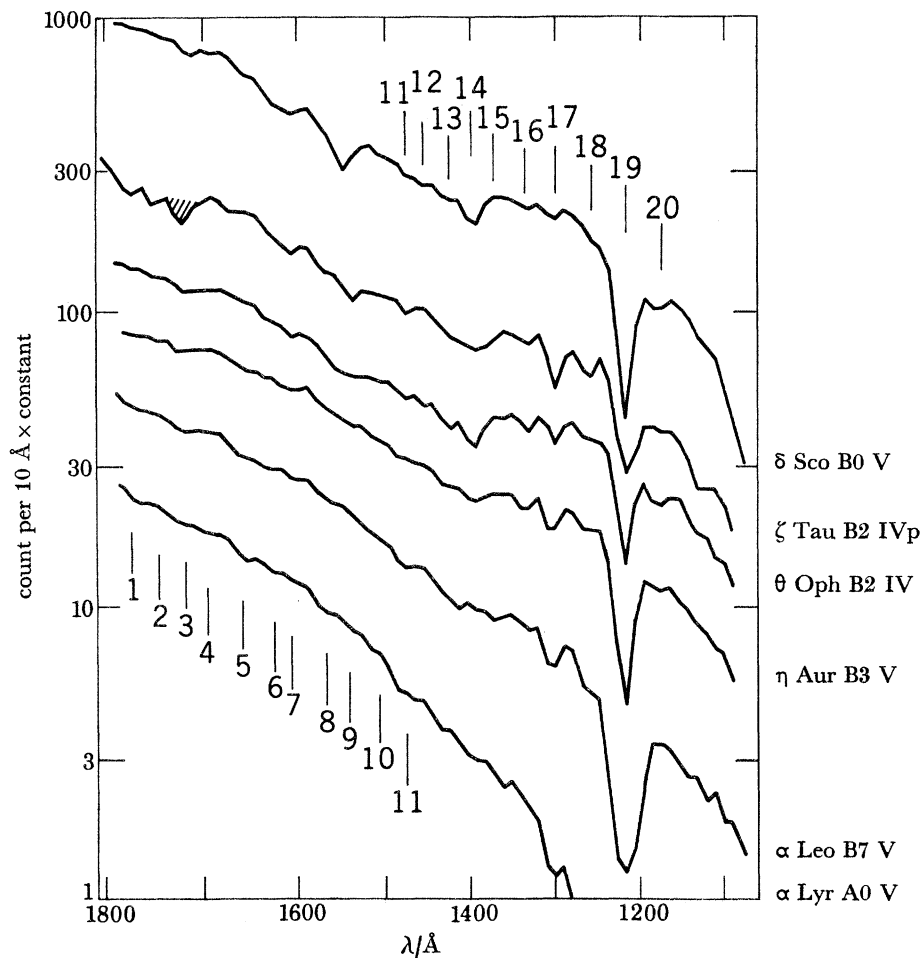


FIGURE 1. OAO-2 spectrum scans of five early-type main-sequence stars and the shell star ζ Tau. Counting rates in a 10 Å band are multiplied by an arbitrary constant and plotted logarithmically against wavelength. Twenty prominent features are indicated.

2. THE ULTRAVIOLET SPECTRUM OF η CANIS MAJORIS, B5Ia

The ultraviolet spectrum of η Canis Majoris, B5Ia, has been scanned with OAO-3, Copernicus, and many absorption lines appear. This spectrum has been studied as representative for B-type supergiants. Spectrum scans are available from 1008 to 1425 Å taken with the U2 spectrometer (Rogerson *et al.* 1973) at 0.2 Å resolution and from 1890 to 3105 Å taken with the

V2 spectrometer at 0.4 Å resolution. The background is a count of 200–300 per dwell interval (13.76 s) on the U2 scan but several thousand on the V2 scan. All absorption lines were listed and they have been identified by comparison with the *Finding list of the Ultraviolet multiplet tables* (Moore 1950, 1952, 1962) and with a list of *Atomic and ionic emission lines below 2000 Å – hydrogen through krypton* prepared by Kelly & Palumbo (1973).

Study of the spectral region 3187–6678 Å and the ultraviolet spectrum scans shows that the spectra listed in table 1 are present. The spectrum is full of lines in the ultraviolet where it is

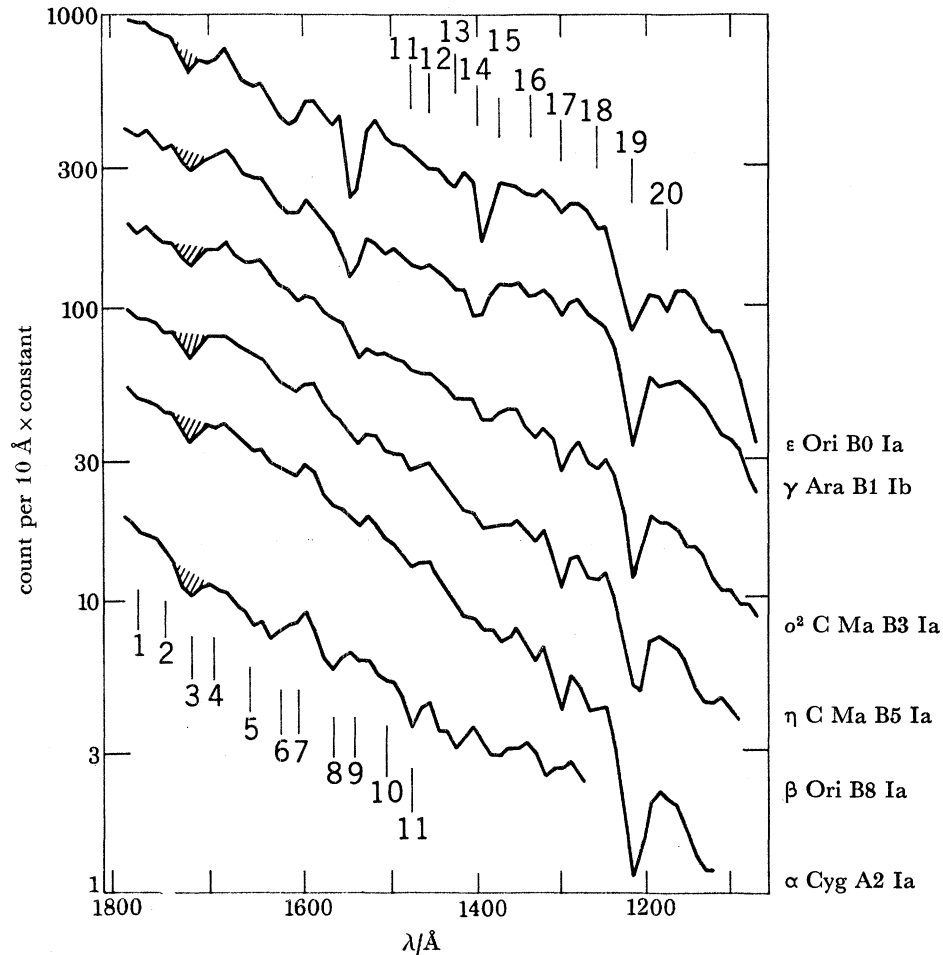


FIGURE 2. OAO-2 spectrum scans of six early-type supergiants. Counting rates in a 10 Å band are multiplied by an arbitrary constant and plotted logarithmically against wavelength. Twenty prominent features are indicated. The cross-hatch feature near 1720 Å occurs only in supergiants and the shell star ζ Tau.

TABLE 1. SPECTRA PRESENT IN η CANIS MAJORIS

definitely present	possibly present
H I, He I, C II, C III	B II, Si I, P III
N I, N II, O I, O II	Cl I, Cl III
Ne I, Na I, Mg I, Mg II	Sc III, Ti IV
Al II, Al III, Si II, Si III, Si IV	Cr IV, Mn IV
P II, S II, S III, S IV	Ni II, Ni III
Cl II, Ca II, Ti III, V III	Y III
Cr II, Cr III, Mn III, Fe II, Fe III	

dominated by lines of the second and third spectra of the metals. A typical spectral region is shown in figure 3. The estimated level of the continuous spectrum and of the background due to stray light and to noise are indicated. Almost every feature can be identified as a line in the second or third spectrum of the metals. In the ultraviolet of B-type supergiants the density of lines is like that in the visible spectral region of an F-type star. The line blocking factor averages 0.5 between 1000 and 1400 Å, 0.2 between 1900 and 2500 Å and 0.1 between 2500 and 3000 Å.

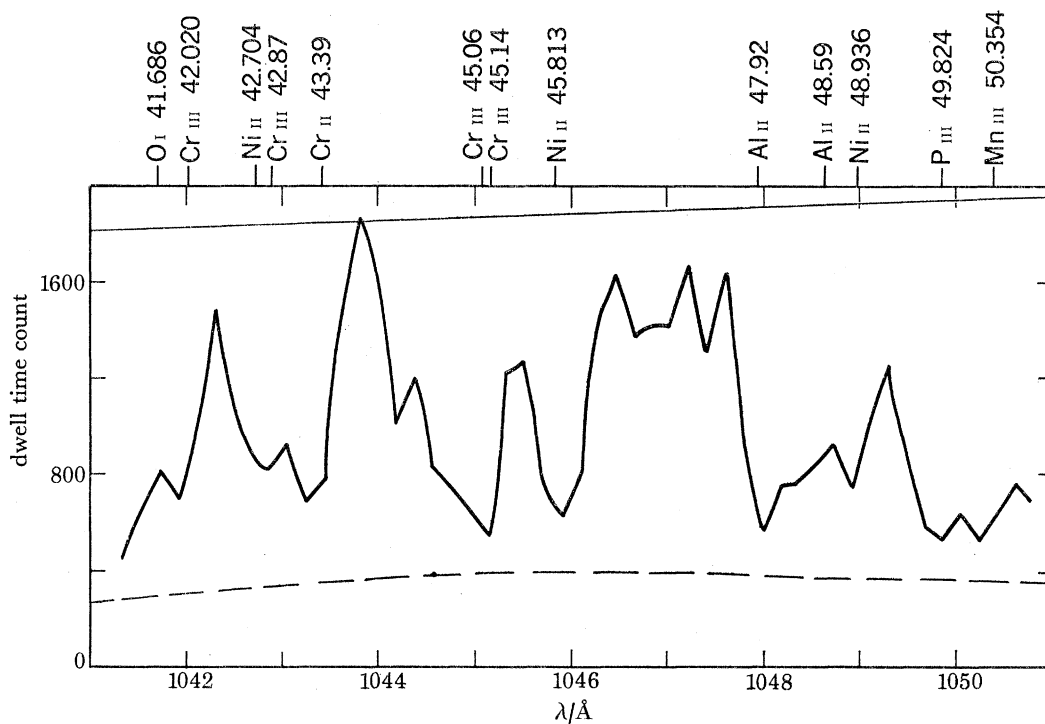


FIGURE 3. The spectrum of η CMa between 1041 and 1051 Å. A continuum level has been estimated by joining the highest points in the spectrum. The level of the stray light and background noise is indicated by a broken line.

In addition to the many lines of the metals, the resonance lines of the spectra of the light elements are present as strong absorption lines indicating outward streaming gas but the strong absorption line from the C III blend at 1176 Å which has a lower excitation potential of 6.5 V is not shortward displaced. The profiles of the C II blend at 1335 Å and the C III blend at 1176 Å are shown in figure 4. The level of the continuous spectrum has been estimated by joining high points in the spectrum while the level of the stray light and noise is estimated using the procedure developed by York *et al.* (1973). These strong lines are broader and deeper than the lines due to the metals, typical profiles of which are shown in figure 3. The strong lines shortward of C III 1176 Å are Cr III 1173.34 Å and a blend of Si III 1172.529 Å and Mn III 1172.721 Å.

In the part of the spectrum of η Canis Majoris accessible to observation one finds well developed resonance lines of H I, C II, N II, Na I, Mg I, Mg II, Si IV, Ca II and Fe II. The profile of Lyman α is so broad on the present spectrum scans that nothing can be said about the profile. The resonance lines due to C II, N II, Mg II and Si IV are shortward displaced by about 120 km s⁻¹, those due to Na I are displaced 25 km s⁻¹ shortward while those due to Mg I,

Ca II and Fe II are not displaced. The Mg II resonance lines are double, consisting of a moderately strong shortward displaced component and a strong stationary component. The lines from excited levels have zero displacement. Crudely it seems that η Canis Majoris is surrounded by a stationary atmosphere and by an expanding atmosphere. The presence of resonance lines of Na I and Mg I in this supergiant atmosphere which corresponds to a level of excitation typical of a temperature near 18000 K is curious. In order to investigate this further, line profiles for the resonance lines have been predicted using a representative model atmosphere and a simple theory of line formation.

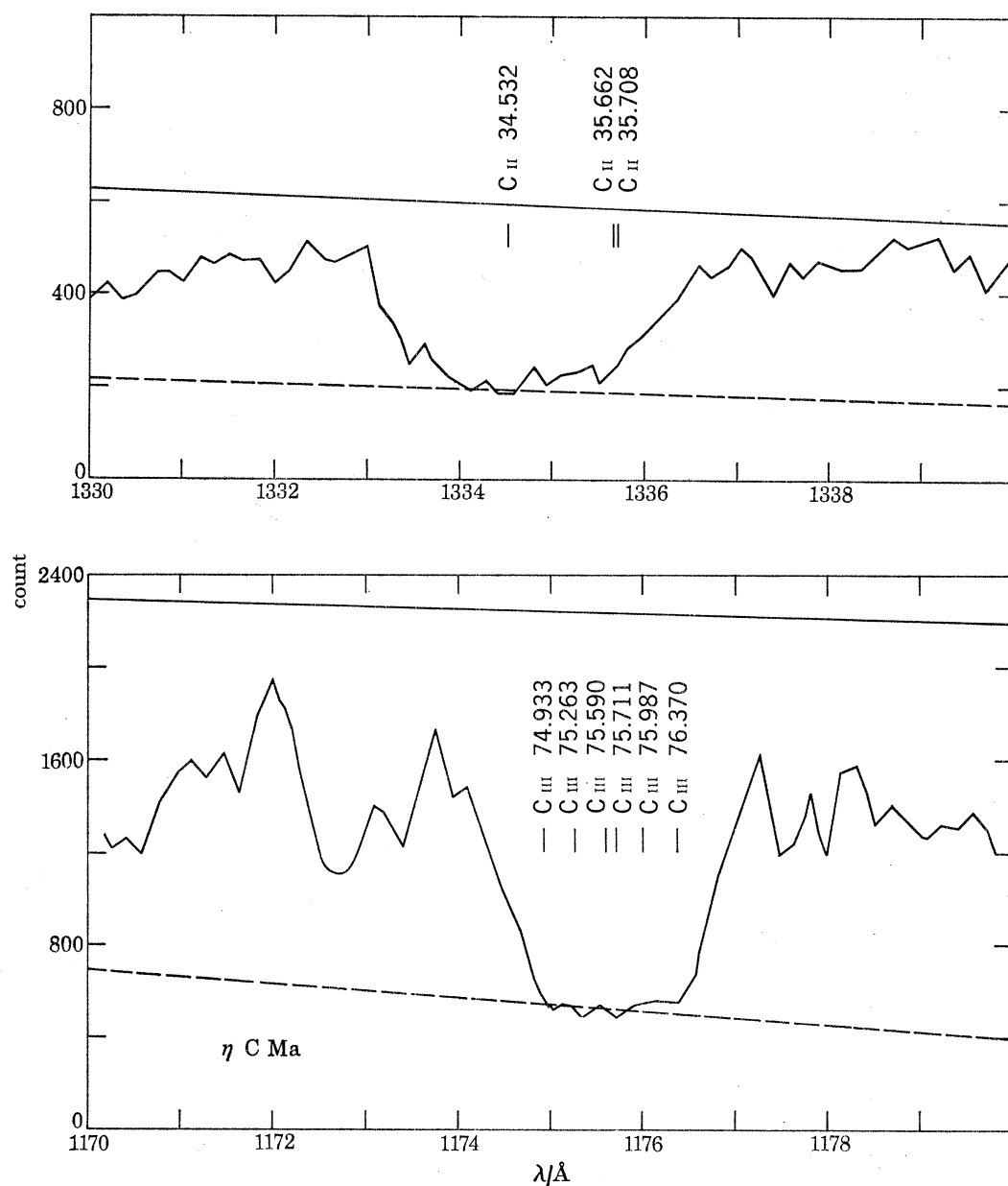


FIGURE 4. The observed profiles of the C II blend at 1334–1335 Å and the C III blend at 1175–1176 Å.

3. A MODEL ATMOSPHERE FOR η CANIS MAJORIS

A coarse analysis of the part of the spectrum of η Canis Majoris accessible to ground-based telescopes by Underhill & Fahey (1973) has shown that the non-l.t.e. model atmospheres computed by Mihalas (1972) with $T_{\text{eff}} = 17500$ K, $\lg g = 2.5$ and with $T_{\text{eff}} = 20000$ K, $\lg g = 2.5$ are representative for those parts of the atmosphere significant for forming the observed spectrum. Curve-of-growth analysis indicates that the motion broadening of the lines can be accounted for by a microturbulence of 15 km s^{-1} . These conclusions have been confirmed by comparison of the profiles and equivalent widths of Si II and Si III lines with values predicted by Lucas W. Kamp who used a realistic model atom and solved simultaneously the equations of statistical equilibrium and radiative transfer. Comparison of Kamp's results with observation indicates that the best representation of the subordinate Si II and Si III lines would be obtained using a non-l.t.e. model with $T_{\text{eff}} = 18000$ K, $\lg g = 2.5$ and a microturbulence of 7.5 km s^{-1} . For the purposes of a first look at the expected resonance line spectrum of η Canis Majoris we have adopted the Mihalas model with $T_{\text{eff}} = 17500$ K, $\lg g = 2.5$, a microturbulence of 15 km s^{-1} and l.t.e. line formation theory. The latter theory was adopted because a simple theory of line formation is required in order to apply it to many lines. It is known that l.t.e.

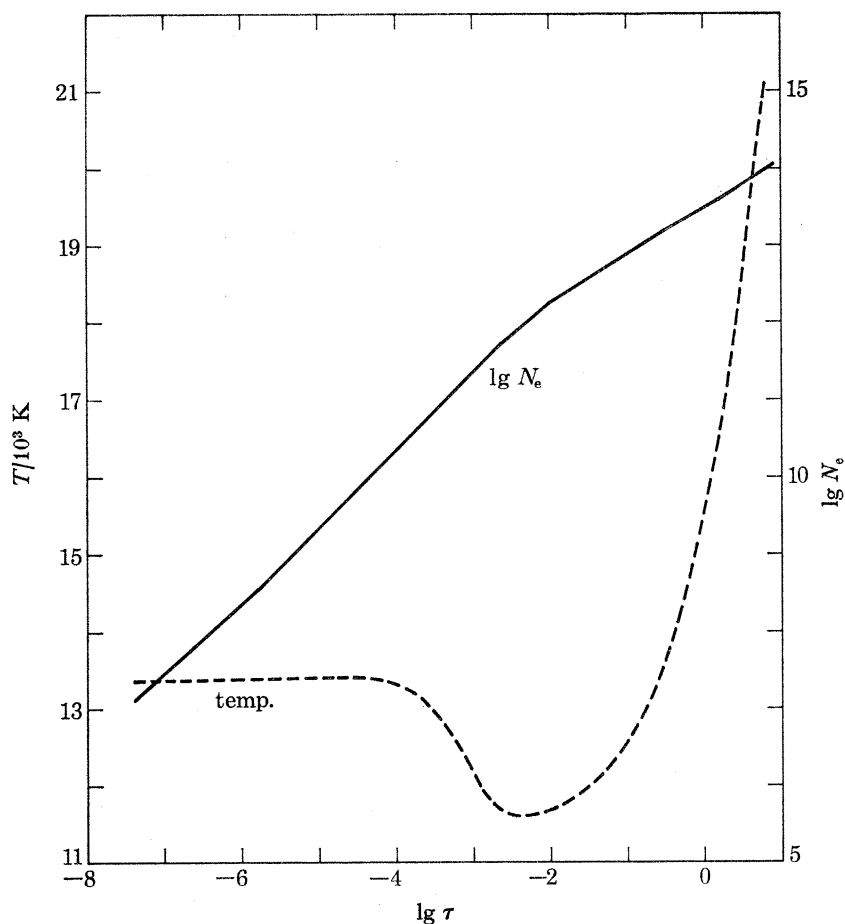


FIGURE 5. The temperature and electron density structure in the outer layers of the Mihalas model with $T_{\text{eff}} = 17500$ K and $\lg g = 2.5$.

theory gives a reasonable representation of the formation of resonance lines except at the line centre where correct theory predicts a deeper line core.

The temperature and electron density structure of the adopted model atmosphere is shown in figure 5. Depth in the atmosphere is measured in terms of τ , the monochromatic optical depth at 3166.66 \AA in the continuous spectrum. Non-l.t.e. effects in the radiative transfer of the hydrogen spectrum cause a temperature rise and plateau in the outer part of the atmosphere. The wings of absorption lines and the continuous spectrum are formed at layers near $\tau = 1$ while the cores of the strong lines are formed in the layers where $\tau \leq 10^{-4}$. Here N_e lies between 10^7 and 10^{10} . The Balmer series breaks off at $n = 24$ which suggests N_e is 10^{12} – 10^{13} in the part of the atmosphere where the wings of the Balmer lines are formed, which is in agreement with the predictions of the model atmosphere.

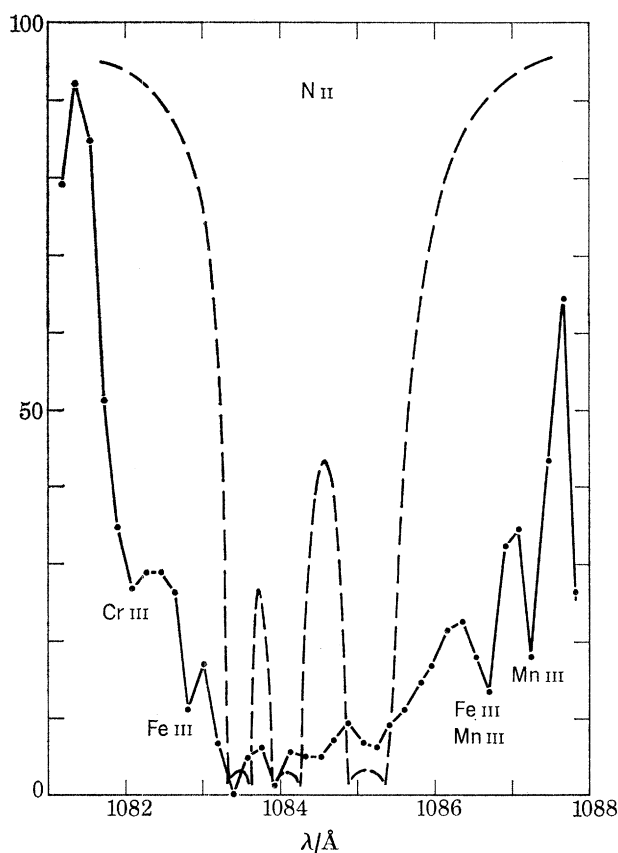


FIGURE 6. The observed and computed profiles of the N II blend at 1084 \AA .

Profiles for resonance lines formed in the adopted model atmosphere have been computed using an l.t.e. theory of line formation. Solar abundances and the gf and I_{rad} values listed by Morton & Smith (1973) were used. The microturbulence is 15 km s^{-1} . This factor allows for some effective broadening of the line absorption coefficient due to motion of the gas in the stellar atmosphere. For the C III blend at 1176 \AA the gf values of Weise, Smith & Glennon (1966) were used; the radiation damping constant was put equal to A_{ki} for each C III line.

The observed and computed profiles of the N II 1084 \AA blend are shown in figure 6. There are six N II lines blending which the computations show as three lines. Lines of Cr III, Fe III and Mn III blend in the wings. The small emission peaks shown in the centres of the predicted

N II lines are artefacts of the l.t.e. line formation theory and the adopted model. They reflect the temperature rise in the outer layers of the adopted model atmosphere. This comparison shows reasonable agreement between theory and observation.

The observed and computed profiles of C III 1176 Å are shown in figure 7. Six lines blend to form the observed feature. Small emission peaks due to the outward temperature rise in the model atmosphere appear. The agreement between theory and observation is generally good indicating that the model is representative of line formation in those parts of the atmosphere of η Canis Majoris contributing to the formation of C III 1176 Å. This line is not shortward displaced.

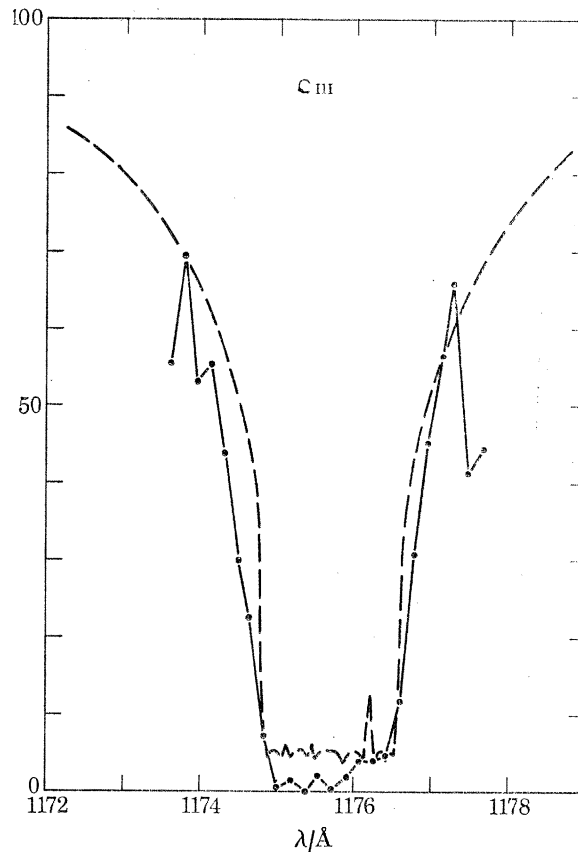


FIGURE 7. The observed and computed profiles of the C III blend at 1176 Å.

The observed and computed profiles of the C II 1335 Å blend are shown in figure 8. The predictions show two lines partially resolved. The emission peaks in the centre of each line are quite conspicuous. The agreement in width between the observed and computed profiles indicates that the major broadening agents in the atmosphere have been accounted for accurately.

The observed and computed profiles of the Si IV resonance lines are shown in figure 9. The computations were done by L. W. Kamp using non-l.t.e. theory. The observations do not show the relatively sharp, deep core which is predicted. Optical depth unity in the line centre is reached near $\lg \tau (3166.66 \text{ Å}) = -3$, thus the centres of these lines are formed in somewhat deeper layers than the l.t.e. calculations indicate for the centres of the N II, C II and C III lines which are formed between $\lg \tau (3166.66 \text{ Å}) = -4$ and -5 .

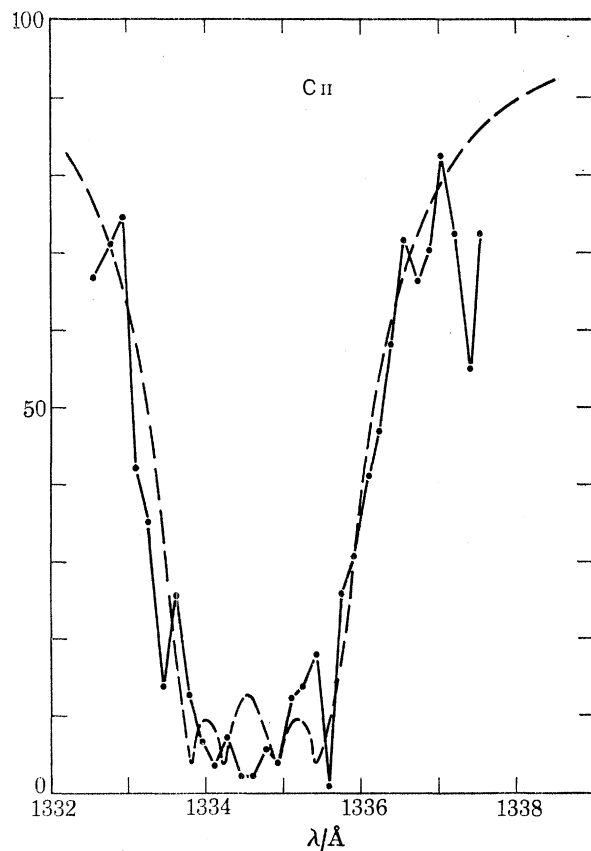


FIGURE 8. The observed and computed profiles of the C II blend at 1335 Å.

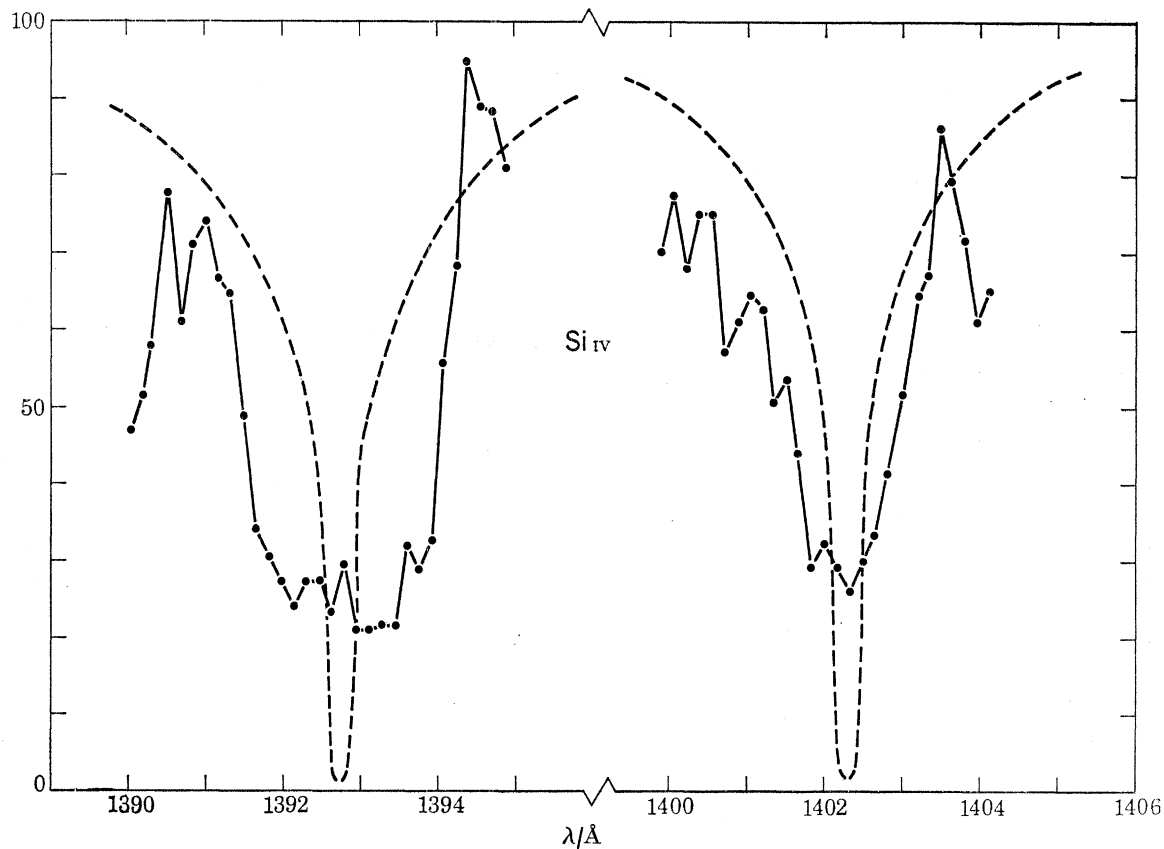


FIGURE 9. The observed and computed profiles of the Si IV resonance lines.

The observed and computed profiles of the Mg II resonance lines are shown in figure 10. The observed lines are double, being composed of a displaced component and a strong stationary component. The predicted profiles agree reasonably well with the displaced components. Optical depth unity in the line centre is reached near $\lg \tau (3166.66 \text{ \AA}) = -3$. The adopted model does not produce Mg II resonance lines as strong as the observed undisplaced components.

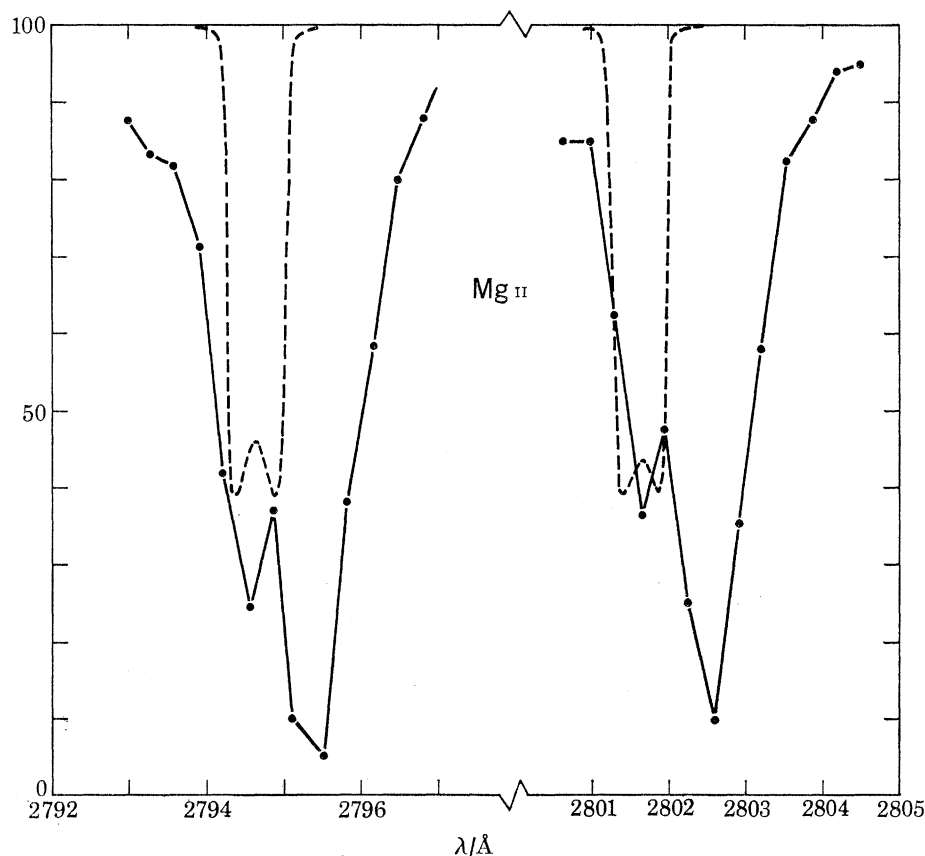


FIGURE 10. The observed and computed profiles of the Mg II resonance lines.

The Mg I resonance line is shown in figure 11. The predicted line has zero intensity, thus the observed line must be coming from a body of gas different from what is included in the model. This line is not shortward displaced; the circumstellar shell which gives rise to the line is stationary with respect to the star so far as can be determined. The observed Ca II K-line and the Na I D-lines are shown in figure 12. The predicted Ca II K-line is shown by a broken line. The predicted D-lines have zero strength; Na I D2 is severely blended with a C II line. The observed Ca II line is weaker than one would expect for an atmosphere like the model, but the Na I lines are anomalously strong. They are shortward displaced by 25 km s^{-1} . Probably the Na I lines are formed in the circumstellar shell which gives rise to the Mg I line. Marschall & Hobbs (1972) have shown that the true interstellar line due to Ca II K is very weak. Inspection of the spectrograms suggests that the interstellar line is the cause of the longward wing observed on the Ca II K profile.

Profiles of the resonance lines of Fe II shown on the OAO-3 V2 tracings do not appear different from the profiles of other metal lines. The Fe II lines are formed in a stationary

layer which may be the same as that revealed by the Mg I and Na I D-lines. It is planned to observe some of the Fe II lines at high resolution in order to see if there is evidence of a sharp component due to a circumstellar, stationary shell as well as a component due to the stationary lower atmosphere of the star which gives rise to most of the lines in the stellar spectrum.

Equivalent widths and line profiles of the Fe II lines listed in table 2 have been computed and compared with the observed profiles. The observed equivalent widths are very uncertain because they depend on the estimated level of the continuous spectrum and of the noise. On

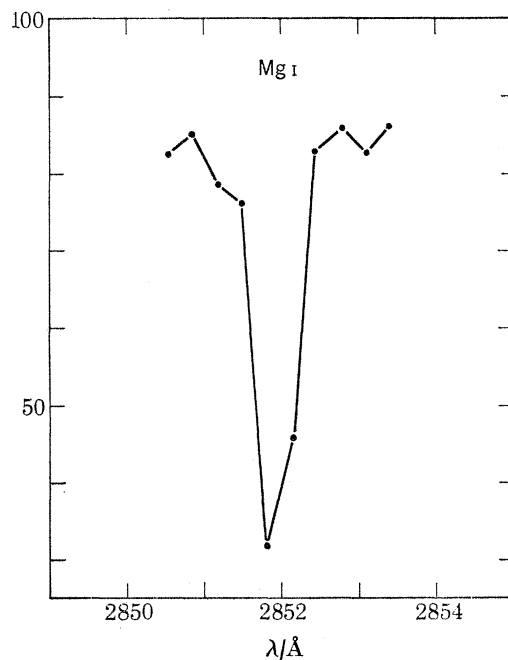


FIGURE 11. The observed profile of the Mg I resonance line.

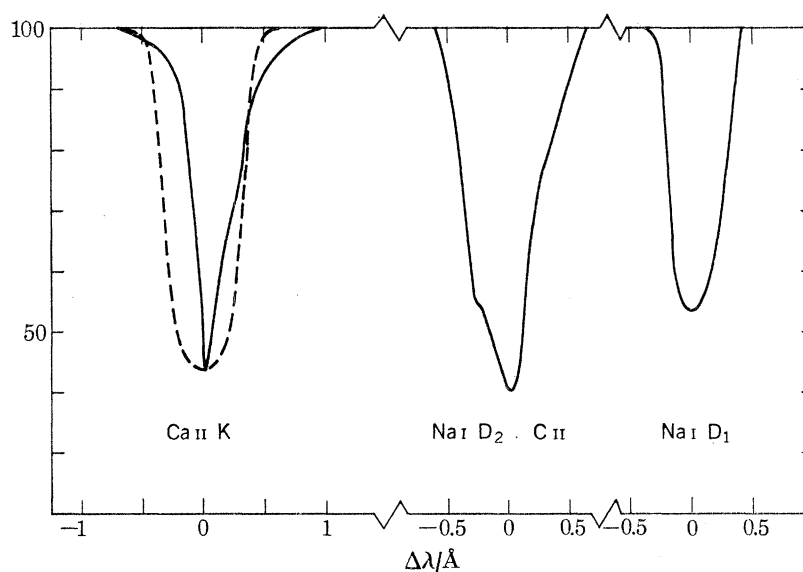


FIGURE 12. The observed profiles of Ca II K- and the Na I D-lines. The predicted K-line is shown by a broken line.

the average the observed lines are 1.7 times as strong as the computed lines for the (17500 K, $\lg g = 2.5$) model, which suggests that there is a component present from the stationary cool shell. The present observations do not have adequate resolution to separate such circumstellar components from the component formed deep in the stellar atmosphere. The computations indicate that the centres of the Fe II lines are formed near $\lg \tau (3166.66 \text{ \AA}) = -1$.

TABLE 2. STRONG Fe II LINES IN η CANIS MAJORIS

wavelength \AA	multiplet	E.P./ cm^{-1}	predicted $W/\text{\AA}$		observed $W/\text{\AA}$
			17500, 2.5	20000, 2.5	
2373.73	2	0.00	0.288	0.149	0.385
2382.03	2	0.00	0.388	0.288	0.708
2388.63	2	384.77	0.312	0.184	0.538
2395.42	2	667.64	0.437	0.295	0.660
2395.63	2	384.77			
2585.88	1	0.00	0.308	0.179	0.592
2598.37	1	384.77	0.682	0.452	1.288
2599.40	1	0.00			

4. DISCUSSION

The adopted model atmosphere and the l.t.e. theory of line formation gives a surprisingly good representation of what is observed in the spectrum of η Canis Majoris. The ultraviolet resonance lines show that the layers between $\tau = 10^{-6}$ and $\tau = 10^{-2}$ are moving outward at about 120 km s^{-1} . Since this velocity does not exceed the escape velocity from the star, the material can be expected to slow down and form a stationary, or nearly stationary shell around the star. Such a shell is visible in the Mg I, Mg II and Na I resonance lines. It does not appear in Ca II. This circumstellar shell will tail off into the interstellar medium. It is planned to investigate this shell further by means of high resolution scans of selected resonance lines in the spectrum of η Canis Majoris.

The resonance lines due to C II and N II and the lines contributing to the C III blend at 1176 \AA are strong enough to lie on the damping part of the curve of growth, thus the predicted results are sensitive to the adopted value for the damping constant. Numerical experiments with values for Γ greater than Γ_{rad} (to simulate possible Stark broadening) showed that the best fit to the observations was obtained when only radiation damping was considered. Stark broadening is not probable at the low densities of a supergiant atmosphere. The width of the core of the C II and C III blends as well as the widths of the Mg II lines are surprisingly well represented by the adopted microturbulence which suggests that the adopted microturbulence represents fairly well the field of motion in the atmosphere of η Canis Majoris. The observed profiles of the Si IV resonance lines are, however, significantly wider than the computed profiles. At 1400 \AA the velocity corresponding to 1 \AA is 214 km s^{-1} . Taken at their face value the observed widths of the Si IV profiles suggest motions of the order of 200 km s^{-1} . This result contradicts the inferences about motion in the stellar atmosphere to be drawn from other well observed lines in the spectrum of η Canis Majoris. The sensitivity of the OAO-3 scanner is not high near 1400 \AA and it is possible that the Si IV line profiles suffer from larger random counting errors than appear to be present in the other lines. Resolution of this contradiction must await more observations.

The observed Fe II lines from multiplets 1 and 2 are about 1.7 times stronger than the predicted lines using the (17500 K, $\lg g = 2.5$) model atmosphere which suggests that higher resolution observations will show Fe II components from the stationary shell. It may be possible to estimate the level of excitation in the stationary shell from the relative strength of Fe II lines from zero voltage levels and from excited levels when observation at high resolution are available.

The ultraviolet spectrum of η Canis Majoris confirms the conclusions drawn from a study of the visible spectrum (Underhill & Fahey 1973) that the atmosphere of this B5Ia supergiant can be well represented by the non-l.t.e. model atmosphere of Mihalas (1972) having $T_{\text{eff}} = 17500$ K and $\lg g = 2.5$. At type B5 there is no evidence for an atmosphere moving outward at a velocity greater than the escape velocity in contrast to the situation found at type B0Ia and earlier.

5. AN INTERPRETATION OF THE CIRCUMSTELLAR LINES

Strong absorption lines are seen at the undisplaced position of Mg II 2795.523 Å, Mg II 2802.698 Å and Mg I 2852.120 Å, and displaced 25 km s⁻¹ shortward of Na I 5889.923 Å and Na I 5895.953 Å. These lines have equivalent widths of 1.10, 0.91, 0.30, 0.32 and 0.18 Å respectively. They may be attributed to absorption in a nearly stationary shell surrounding η Canis Majoris or to absorption in the interstellar medium between the star and the observer. In order to determine whether these lines might be interstellar in origin, the observed equivalent widths were used to enter the curve of growth for interstellar lines and derive a column density. The simplest case was considered, namely a single cloud in which the velocity distribution of the atoms was described by a temperature of 100, 1000 and 7000 K and the damping was pure radiation damping. The line at 5890 Å is a blend of C II (formed in the stellar atmosphere) and Na I. Consequently, its equivalent width gives an upper limit to the column density of neutral Na. The results are given in table 3.

TABLE 3. ESTIMATED COLUMN DENSITIES (ATOMS cm⁻²)

line	$T = 100$ K	$T = 1000$ K	$T = 7000$ K
Mg I 2852 Å	3.1×10^{15}	3.1×10^{15}	2.7×10^{15}
Mg II 2796 Å	1.5×10^{17}	1.4×10^{17}	1.3×10^{17}
Mg II 2803 Å	2.0×10^{17}	1.9×10^{17}	2.1×10^{17}
Na I 5890 Å	2.4×10^{15}	2.4×10^{15}	1.3×10^{15}
Na I 5896 Å	1.5×10^{15}	1.3×10^{15}	4.8×10^{13}

The total column density of Mg atoms and ions is found by adding the results for Mg I and Mg II. (This assumes that the number of Mg atoms or ions in excited states is negligible.) If it be assumed that the relative abundance of Na to Mg is the solar value (Allen 1963), the total column density of Na may be estimated. Finally, by assuming solar abundances, relative to hydrogen the column density of hydrogen may be estimated. For temperatures of 100, 1000 and 7000 K the results are 6.2×10^{21} , 5.8×10^{21} and 5.9×10^{21} cm⁻² respectively.

If it is assumed that the visual absolute magnitude of a B5Ia star is -7.0 and that the E_{B-v} of η Canis Majoris is 0.09, corresponding to an extinction of 0.27 magnitudes, the distance to η Canis Majoris is 2.1×10^{21} cm. If the Mg I, Mg II and Na I lines are interstellar in origin the average line-of-sight density of hydrogen is 3.0, 2.8 and 2.8 cm⁻³ for velocity dispersions corresponding to 100, 1000 and 7000 K. These densities are approximately ten times the normal

hydrogen density in interstellar space. Thus, the assumption that the observed lines are interstellar in origin is untenable. The observed Mg I, Mg II and Na I lines must be formed in a circumstellar shell. It is logical to conclude that this circumstellar shell is created by the slowing down of the outward moving gas which is seen in the shortward displaced lines due to C II, N II, Si IV and Mg II.

The B3Ia supergiant α^3 Canis Majoris which has a spectrum rather like that of η Canis Majoris does not have strong Na I D-lines in its spectrum (Van Helden 1972). Probably it is not surrounded by a cool circumstellar shell like η Canis Majoris.

I am grateful to Dr Lyman Spitzer and Dr D. C. Morton for permission to work on the OAO-Copernicus tracings of the spectrum of η Canis Majoris. The line profiles were calculated using a program developed by D. Fischel, J. Fowler and A. Karp to synthesize spectra from a model atmosphere. A.B.U. is Guest Investigator with the Princeton University telescope on the Copernicus satellite, which is sponsored and operated by the National Aeronautics and Space Administration.

REFERENCES (Underhill)

- Allen, C. W. 1963 *Astrophysical quantities*, p. 30. London: Athlone Press.
- Kelly, R. L. & Palumbo, L. J. 1973 *Atomic and ionic emission lines below 2000 Å - hydrogen through krypton*. NRL Report 7599. Washington, D.C.: U.S. Government Printing Office.
- Lamers, H. J. 1972 *Astron. & Astrophys.* **17**, 34-40.
- Marschall, L. A. & Hobbs, L. M. 1972 *Astrophys. J.* **173**, 43-62.
- Mihalas, D. 1972 *Non-LTE model atmospheres for B and O stars*. NCAR-TN/STR-76.
- Moore, C. E. 1950 An ultraviolet multiplet table. *Circ. U.S. natn. Bur. Stand.* 488, section 1.
- Moore, C. E. 1952 An ultraviolet multiplet table. *Circ. U.S. natn. Bur. Stand.* 488, section 2.
- Moore, C. E. 1962 An ultraviolet multiplet table. *Circ. U.S. natn. Bur. Stand.* 488, section 4.
- Morton, D. C., Jenkins, E. B. & Bohlin, R. C. 1968 *Astrophys. J.* **154**, 661-676.
- Morton, D. C. & Smith, W. H. 1973 *Astrophys. J. Suppl.* no. 233.
- Rogerson, J. B., Spitzer, L., Drake, J. F., Dressler, K., Jenkins, E. B., Morton, D. C. & York, D. G. 1973 *Astrophys. J. Lett.* **181**, L97-L102.
- Underhill, A. B. & Fahey, R. P. 1973 *Astrophys. J. Suppl.* **25**, 463-486.
- Van Helden, R. 1972 *Astron. & Astrophys.* **21**, 209-222.
- Weise, W. L., Smith, M. W. & Glennon, B. M. 1966 *Atomic transition probabilities*, vol. 1, NSRDS-NBS4.
- Wilson, R. 1958 *Pub. R. Obs. Edinburgh* **2**, no. 3.
- York, D. G., Drake, J. F., Jenkins, E. B., Morton, D. C., Rogerson, J. B. & Spitzer, L. 1973 *Astrophys. J. Lett.* **182**, L1-L6.